

## Selenium-capped cyclic peptide nanoparticles for penicillamine drug delivery: A DFT Study

Sara Moghimi, Ali Morsali\* & Mohammad M Heravi

Department of Chemistry, Mashhad Branch, Islamic Azad University, Mashhad 917 568, Iran

Email: almorsali@yahoo.com/ morsali@mshdiau.ac.ir

Received 18 October 2018; revised and accepted 20 December 2019

Using a model for performance of penicillamine (PCA) anti-cancer drug on selenium-cyclic peptide nanoparticle (CPSeNP), 11 noncovalent configurations have been investigated. Se8 ring model and cyclooctaglycine have been used for selenium nanoparticle (SeNP) and cyclic peptide (CP), respectively. Binding energies, quantum molecular descriptors and solvation energies have been studied in gas phase and water at M06-2X /6-31G\*\* level of theory. The calculated energies represent the high-energy stability of CPSeNP/PCA 1-11 configurations. Solvation energies showed that drug solubility increases, which is a major factor for their use in drug delivery. Regarding to quantum molecular descriptors such as hardness and electrophilic power, the drug reactivity increases in the vicinity of SeNP. The QTAIM analysis revealed that intramolecular interaction Se-L (L =O, H, S, C, N) plays an important role in the system. Se-L interaction in all configurations is relevant to weak interactions. The configurations that PCA drug is located in parallel with the carrier (CPSeNP) are more stable than penicillamine-CP or penicillamine-SeNP systems.

**Keywords:** Selenium nanoparticle, Cyclic peptide, Penicillamine, Drug delivery, Density Functional Theory (DFT)

Effective delivery of drug toward target sites will significantly improve their therapeutic effectiveness. Drug delivery systems have been recently mentioned as new tools for improving drug efficacy<sup>1,2</sup>. Iron oxide NPs<sup>3</sup>, Silica NP<sup>4</sup>, Gold NPs<sup>5</sup> and other mineral NPs<sup>6</sup> have been studied to reduce toxicity and increase biocompatibility and stability. Nanoscientists use a broad range of biomedical applications of nanoparticles, with regard to their chemical stability, environmental compatibility, high mechanical resistance and strength to bacterial attacks<sup>7-9</sup>.

Cyclic peptide have many applications in different fields such as drug delivery, nanoscience, optical sensors, and electronic devices<sup>10-13</sup>. The cyclic structure of these compounds with various chain amino acids is a good model for encapsulation of drugs<sup>14</sup>. Cyclic structure is made by the terminus of a peptide attached to another part of the peptide with an amide bond. In comparison to synthetic molecules, peptides have less toxicity, so they don't aggregate in the tissue. Drugs based on cyclic peptides can be less harmful. Due to the higher stability of configuration, the cyclic peptides have usually better biological activities in comparison to similar types of linear peptides.

Cyclic peptides have various structural features that allow them to be used as connectors of target

drugs in medical applications. The studies showed that intracellular adsorption can be impressively enhanced in the presence of cyclic peptide containing *arginine* and *tryptophan*<sup>15-17</sup>. Penicillamine is used for genetic disorder related to copper metabolism (Wilson disease)<sup>18,19</sup>. In addition, it is used as an anticancer factor. Recent studies have shown the inhibition of the growth of various cancerous cells<sup>20</sup>. The thiol group exhibits high permeability to cancerous cells due to its high reactivity in its structure and has a high rate in removal of cancerous cells and can strongly connect to blood protein for delivery of penicillamine into cancerous cells<sup>20,21</sup>. It has been reported that poly( $\alpha$ )-L-glutamic acid PCA (PGA-PCA) system, increases the permeability of penicillamine into cancerous cells<sup>22,23</sup>.

The potential application of nanotechnology in the development of new drug delivery systems (DDSs) is under consideration<sup>24-26</sup>. Drug delivery systems based on nano-DDS have several advantages over larger DDSs, such as lower toxicity and improved cellular absorption. Peptides are commonly used as nano-scale systems for drug delivery, due to their ability to carry a wide range of molecules through the encapsulation of the drug. In addition, peptides are used as a part of the nanoscale structure DDS by a wide range of amino acids with different physio-chemical properties. For

example, functionalized peptides with gold nanoparticles have been used as one of the previous biochemical systems for drug delivery and the improvement of cellular delivery of several drugs by noncovalent complexation<sup>17,27,28</sup>. Among various metal nanoparticles, selenium nanoparticles (SeNPs) have not been studied very much. Selenium is a necessary element that is daily absorbed from the diet (55  $\mu\text{g}$ ). Also, selenium is essential for cellular function. A high dose of selenium can cause cell death<sup>29</sup>. So, new functionalized SeNPs are needed which can be used as non-toxic nano DDS<sup>30</sup>. Functionalized SeNPs with other compounds improve their biological properties. The size of nanoparticles is a critical factor that can change their biological activity. The consumption and selenium chemical composition is very important for reducing toxicity and increasing therapeutic effects<sup>31,32</sup>.

Quantum studies help to design and analysis of drug delivery systems<sup>33-36</sup>. The Nobel Prize for Chemistry awarded in 2016 was given for the design and manufacture of usable molecular machines in drug delivery<sup>37,38</sup>. In addition to the experimental methods, the quantum chemical methods are important tools for the investigation of drug carrier systems<sup>39-45</sup>. In this study, density functional theory (DFT) was utilized to investigate the functionalization of cyclic peptide-selenium nanoparticles (CPSeNPs) using penicillamine (PCA) anticancer drug.

### Computational methods

DFT calculations are performed using M06-2X<sup>46,47</sup> with Gaussian 09<sup>48</sup> and 6-31G(d,p) basis set. All species have been optimized in gas phase and water. Solvent effects were studied using the (PCM)<sup>49,50</sup> model. Solvation energies ( $\Delta E_{\text{solv}}$ ) were calculated using the following equation.

$$\Delta E_{\text{solv}} = E_{\text{solv}} - E_{\text{gas}} \quad \dots(1)$$

Where  $E_{\text{solv}}$  and  $E_{\text{gas}}$  represent the total energy of solution and gas phase, respectively.

Calculations were performed for penicillamine, cyclic peptide (CP), selenium nanoparticles (SeNPs) systems. Quantum molecular descriptors were used to investigate chemical reactivity and stability. The hardness ( $\eta$ ) shows the resistance versus the electronic structure change.

$$\eta = (I - A)/2 \quad \dots(2)$$

Where  $I = -E_{\text{HOMO}}$ ,  $A = -E_{\text{LUMO}}$ .

The electrophilicity index ( $\omega$ )<sup>51</sup> was obtained from equation (3):

$$\omega = (I + A)^2/8\eta \quad \dots(3)$$

We investigated the hydrogen bond using the QTAIMs calculations. QTAIM calculations are done by the AIMALL software<sup>52</sup>. QTAIM is based on topological parameters such as electron density  $\rho(r)$ <sup>53</sup>. We studied various values of electron density such as  $G_b$  (kinetic energy density),  $V_b$  (potential energy density),  $H_b$  (total energy density), and  $\nabla^2\rho$  (Laplacian of electron density) at a critical point (BCP) to distinguish the nature of the bond in different species.

## Results and Discussion

### Binding and solvation energies

Cyclooctaglycine and Se8 ring model were employed for cyclic peptide (CP)<sup>54</sup> and selenium nanoparticle (SeNP)<sup>55,56</sup>, respectively. Selenium nanoparticle, cyclic peptide and penicillamine drug including SH, OH, CO, NH<sub>2</sub> groups are shown in Fig. 1. The interaction of penicillamine with peptide-

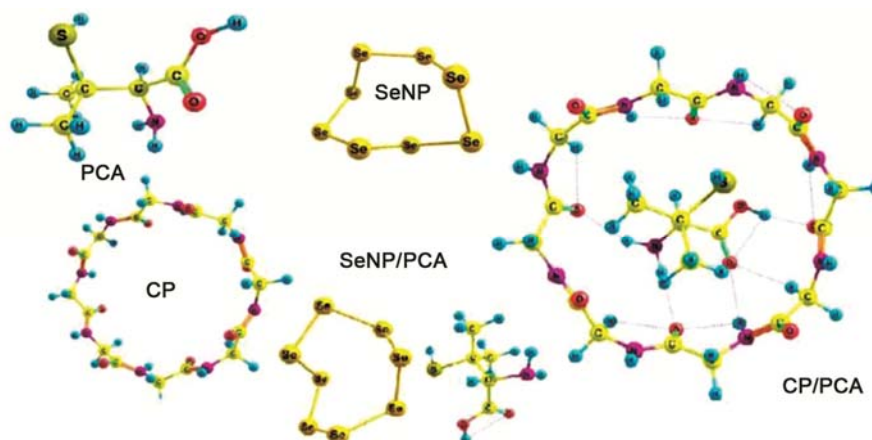


Fig. 1 — Optimized structures of PCA, SeNP, CP, SeNP/PCA and CP/PCA.

selenium nanoparticles has been considered in 11 different ways (CPSeNP/ PCA1–11). The optimized geometries of CPSeNP/ PCA1–11 in aqueous solution at the M06-2X/6-31G \*\* level are shown in the Fig. 2 (see the Supplementary data for the Cartesian coordinates and absolute energies of the calculated structures).

Binding energies ( $\Delta E$ ) were calculated using the following equation:

$$\Delta E = E_{CPSeNP/PCA1-11} - (E_{CP} + E_{SeNP} + E_{PCA}) \quad \dots(4)$$

Where  $E_{CPSeNP/PCA1-11}$ ,  $E_{CP}$ ,  $E_{SeNP}$  and  $E_{PCA}$  are energies of CPSeNP/ PCA1-11, CP, SeNP and PCA, respectively.

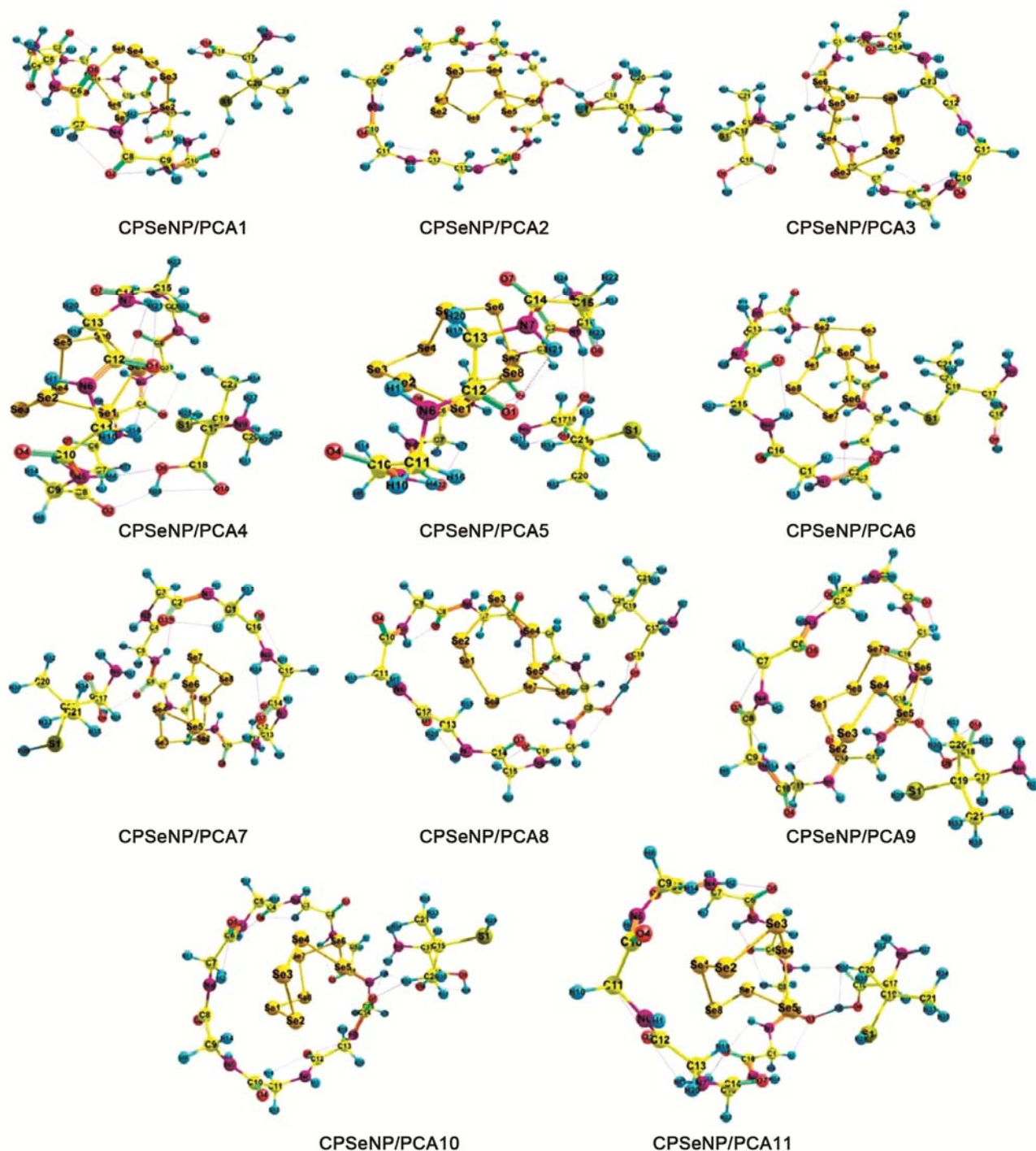


Fig. 2 — Optimized structures of CPSeNP/PCA1-11.

The binding energy values in gas phase and water in M06-2X are shown in Table 1.  $\Delta E$ s depend on the orientation of the drug relative to the CPSeNP. According to both phases, among 11 species, CPSeNP/PCA4 is the most stable chemical structure in which the penicillamine drug stay on in parallel with CPSeNP, and the OH and SH functional groups interact with the functional groups of CPSeNP and the OH bonding is kind of hydrogen bonding (Fig. 2).

Comparison of binding energies shows that the encapsulation of SeNP within the CP increases the binding energy, therefore, PCA can be functionalized on the CPSeNP surface, although this performance is sometimes weaker in aqueous solutions than in the gas phase.

We evaluated the solvation energies for all species (Table 1). The negative values of these energies indicate that the solvation process is spontaneous. The absorption of PCA drug on CPSeNP increases drug solubility, which is an essential factor for its application as an efficient anti-cancer drug.

The drug solubility in the presence of CPSeNP increases from  $-31.34 \text{ kJ mol}^{-1}$  to  $-99.43 \text{ kJ mol}^{-1}$  (mean value of CPSeNP/PCA1–11). The solubility of SeNP increases after activating CPSeNP with PCA medicine, which is very important in drug delivery field. The major reason of increasing PCA and SeNP solubility is the presence of CP.

SeNP solubility increased from  $-9.66 \text{ kJ mol}^{-1}$  to  $-99.43 \text{ kJ mol}^{-1}$  (mean value of CPSeNP/PCA1–11) in the vicinity of CP and PCA. Due to having CO, NH functional groups, CP causes a hydrogen bond

between the PCA drug and CP and the solubility of the CP decreases somewhat.

Therefore, CP in addition to decreasing SeNP toxicity, increases its solubility, which is an important problem in drugs targeted delivery. In fact, these two carriers of CP and SeNP complement each other, and the presence of SeNP improves the binding energy values and CP solubility.

#### Quantum molecular descriptors

In quantum molecular descriptors (both gas phase and water), the  $E_g$  (energy gap between LUMO and HOMO) and  $\eta$  values of CPSeNP/PCA1–11 are approximately the same, as shown in Table 2.  $E_g$  and  $\eta$  values of structure 4 are more than other structures,

Table 2 — Quantum molecular descriptors (eV) for optimized geometries

Species	$E_{HOMO}$	$E_{LUMO}$	$E_g$	$\eta$	$\omega$
H <sub>2</sub> O					
Se	-1.64	-7.18	5.54	2.77	3.51
PCA	1.21	-8.16	9.37	4.68	1.28
CP	1.39	-8.49	9.89	4.94	1.27
CP/PCA	0.99	-7.99	8.99	4.49	1.36
NP/PCA	-1.59	-7.09	5.50	2.75	3.43
CP–SeNPs/PCA1	-1.29	-6.84	5.55	2.77	2.97
CP–SeNPs/PCA2	-1.47	-6.95	5.47	2.73	3.23
CP–SeNPs/PCA3	-1.48	-6.87	5.39	2.69	3.24
CP–SeNPs/PCA4	-1.36	-6.91	5.54	2.77	3.08
CP–SeNPs/PCA5	-1.34	-6.86	5.51	2.75	3.05
CP–SeNPs/PCA6	-1.47	-6.91	5.44	2.72	3.23
CP–SeNPs/PCA7	-1.39	-6.82	5.42	2.71	3.11
CP–SeNPs/PCA8	-1.42	-6.86	5.43	2.71	3.15
CP–SeNPs/PCA9	-1.42	-6.83	5.40	2.70	3.14
CP–SeNPs/PCA10	-1.47	-6.91	5.43	2.71	3.24
CP–SeNPs/PCA11	-1.37	-6.88	5.51	2.75	3.09
Gas					
Se	-1.74	-7.23	5.49	2.74	3.66
PCA	1.34	-8.02	9.36	4.68	1.18
CP	1.34	-8.57	9.91	4.9	1.31
CP/PCA	0.84	-8.03	8.88	4.44	1.45
SeNP/PCA	-1.58	-7.04	5.46	2.73	3.40
CP–SeNPs/PCA1	-1.22	-6.74	5.52	2.76	2.87
CP–SeNPs/PCA2	-1.53	-6.95	5.41	2.70	3.32
CP–SeNPs/PCA3	-1.56	-6.89	5.32	2.66	3.35
CP–SeNPs/PCA4	-1.28	-6.82	5.53	2.76	2.96
CP–SeNPs/PCA5	-1.36	-6.84	5.47	2.73	3.07
CP–SeNPs/PCA6	-1.59	-6.98	5.38	2.69	3.41
CP–SeNPs/PCA7	-1.49	-6.85	5.35	2.67	3.25
CP–SeNPs/PCA8	-1.47	-6.87	5.39	2.69	3.23
CP–SeNPs/PCA9	-1.50	-6.85	5.35	2.67	3.25
CP–SeNPs/PCA10	-1.49	-6.85	5.36	2.68	3.25
CP–SeNPs/PCA11	-1.41	-6.90	5.48	2.74	3.15

Table1 — Binding and solvation energy values ( $\text{kJ mol}^{-1}$ ) for corresponding structures

Species	$\Delta E_{\text{gas}}$	$\Delta E_{\text{H}_2\text{O}}$	$\Delta E_{\text{solv}}$
PCA	–	–	-31.34
CP	–	–	-140.53
SeNP	–	–	-9.66
CP/PCA	-219.86	-113.44	-17.15
SeNP/PCA	-79.53	-75.52	-36.99
CPSeNP/PCA1	-503.80	-464.26	-84.03
CPSeNP/PCA2	-457.63	-445.79	-111.74
CPSeNP/PCA3	-482.54	-470.13	-111.15
CPSeNP/PCA4	-547.60	-497.19	-73.17
CPSeNP/PCA5	-514.59	-494.86	-103.83
CPSeNP/PCA6	-473.85	-461.30	-111.01
CPSeNP/PCA7	-496.95	-470.94	-97.56
CPSeNP/PCA8	-485.08	-462.11	-100.60
CPSeNP/PCA9	-511.93	-494.66	-106.31
CPSeNP/PCA10	-523.83	-495.94	-95.68
CPSeNP/PCA11	-487.92	-463.04	-98.69

which indicates that it is more stable than other structures.  $E_g$ ,  $\eta$  and  $I$  for the drug are greater than those of the CPSeNP/PCA1-11 configurations, which indicates that drug stability in the presence of selenium and cyclic peptide is reduced and its reactivity is increased.

Since electrophilicity is used to predict toxicity, it can be said that the toxicity of SeNP is reduced in the presence of the cyclic peptide and drug. The  $\omega$  values of CPSeNP/PCA1-11 are higher than PCA in both phases, which indicates that the PCA drug plays the role of the electron acceptor.

#### QTAIM analysis

In this section, a comprehensive study about the nature and bonding interactions strength was performed by analyzing critical points of BCP bonding using QTAIM analysis. One of the parameters is electron density ( $\rho(r)$ ), which indicates the strength of a bond, if the amount of  $\rho(r)$  to be large, means that the related bond is stronger. Laplacian electron density ( $\nabla^2\rho$ ) shows the nature of bond. The positive value of  $\nabla^2\rho$  indicates a decrease in electron density for the closed-shell systems such as ion interactions, hydrogen bond and Van der Waals interactions. In contrast to the negative values of  $\nabla^2\rho$  indicate that the electron density is focused in the internuclear region (shared interactions or covalent interactions).

If ( $\nabla^2\rho < 0$ ,  $H_b < 0$ ), ( $\nabla^2\rho > 0$ ,  $H_b < 0$ ) and ( $\nabla^2\rho > 0$ ,  $H_b > 0$ ), interactions will be strong, intermediate and weak, respectively. For the parameter  $-G_b/V_b$ , if  $-G_b/V_b > 1$ ,  $0.5 < -G_b/V_b < 1$  and  $-G_b/V_b < 0.5$ , the character of a bond will be non-covalent, partially covalent, and covalent bonds, respectively<sup>57</sup>.

The structures of CPSeNP/PCA4 and CPSeNP/PCA2 have been reported as the most stable configuration and the most unstable configuration, respectively. The molecular graph for CPSeNP/PCA4 configuration in aqueous solution is shown in Fig. 3. The values of  $-G_b/V_b$ ,  $V_b$ ,  $G_b$ ,  $H_b$ ,  $\nabla^2\rho(r)$ ,  $\rho(r)$  are shown in Table 3. The hydrogen bond energy values are calculated using  $E_{HB} = 1/2V_b$ <sup>58</sup>. Se-Se interactions in SeNP with  $\nabla^2\rho < 0$ ,  $-G_b/V_b < 0.5$ ,  $H_b < 0$  are classified as strong covalent bonds (Table 3).

In the configuration of CPSeNP/PCA4, we face with two categories of important interactions. The first group of interactions is related to SeNP-CP or SeNP-PCA (Se-L; L = O, N, C, S, H) drug. The interactions of Se-L with  $\nabla^2\rho > 0$ ,  $-G_b/V_b < 1$ ,  $H_b > 0$  are related to weak interactions (Table 3). In the most stable configuration, the number and strength of these

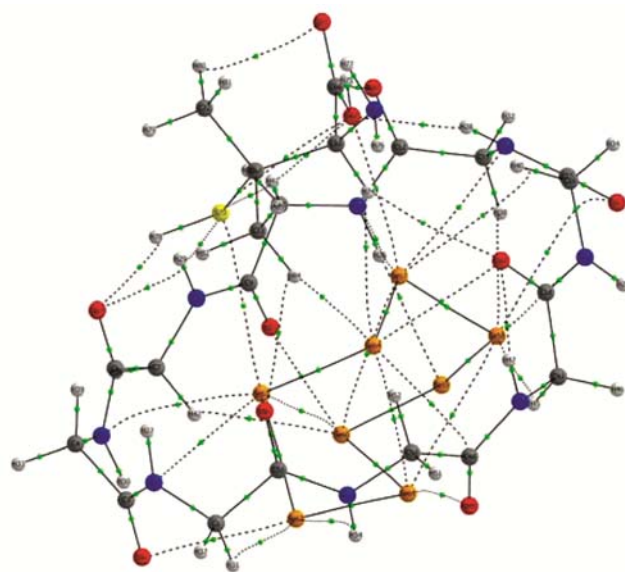


Fig. 3 — QTAIM Molecular graph of CPSeNP/PCA4.

Table 3 — Topological parameters in a.u. for CPSeNP/PCA4

Atoms	$\rho(r)$	$\nabla^2\rho(r)$	$V_b$	$G_b$	$H_b$	$-G_b/V_b$
Se-Se interactions						
Se62 – Se63	0.0951	-0.038659	-0.0736	0.0319	-0.0416	0.43436
Se60 – Se63	0.0161	0.043815	-0.0087	0.0098	0.0011	1.1279
Se57 – Se60	0.0150	0.038784	-0.0076	0.0086	0.0010	1.1309
Se57 – Se58	0.1108	-0.060533	-0.0993	0.0420	-0.0572	0.4238
Se57 – Se64	0.1042	-0.05401	-0.0872	0.0368	0.0009	0.4226
Se61 – Se64	0.0179	0.045099	-0.0094	0.0103	-0.0596	1.0960
Se58 – Se59	0.1018	-0.051119	-0.0834	0.0353	-0.0480	0.4233
Se60 – Se61	0.1062	-0.069832	-0.0874	0.0349	-0.0524	0.4001
Se59 – Se60	0.1128	-0.07667	-0.1000	0.0404	-0.0596	0.4042
Se58 – Se61	0.0164	0.043533	-0.0086	0.0097	0.0011	1.1266
Se61 – Se62	0.1114	-0.073299	-0.0985	0.0400	-0.0584	0.4069

(Contd.)



Table 3 — Topological parameters in a.u. for CPSeNP/PCA4 (Contd.)

Atoms	$\rho(r)$	$\nabla^2\rho(r)$	$V_b$	$G_b$	$H_b$	$-G_b/V_b$
Se-L interactions						
N11 – Se57	0.0126	0.0386	-0.0073	0.0085	0.0011	1.1590
N14 – Se57	0.0116	0.0333	-0.0070	0.0076	0.0006	1.0918
N17 – Se58	0.0142	0.0401	-0.0086	0.0093	0.0006	1.0788
C6 – Se63	0.0144	0.0521	-0.0093	0.0111	0.0018	1.19869
N8 – Se63	0.0089	0.0237	-0.0051	0.0055	0.0004	1.0809
N2 – Se63	0.0126	0.0362	-0.0073	0.0082	0.0008	1.1150
Se57 – Se64	0.1042	-0.0540	-0.0872	0.0368	-0.0503	0.4226
O19 – Se57	0.0101	0.0317	-0.0060	0.0070	0.0009	1.1502
H38 – Se58	0.0112	0.0350	-0.0060	0.0074	0.0013	1.2230
H45 – Se58	0.0108	0.0324	-0.0056	0.0068	0.0012	1.2194
H26 – Se59	0.0148	0.0374	-0.0086	0.0090	0.0003	1.0416
H42 – Se60	0.0116	0.0366	-0.0065	0.0078	0.0013	1.2012
O23 – Se60	0.0191	0.0624	-0.0142	0.0149	0.0006	1.0460
O49 – Se61	0.0146	0.0482	-0.0103	0.0111	0.0008	1.0847
H31 – Se62	0.0101	0.0323	-0.0051	0.0066	0.0014	1.2853
O21 – Se62	0.0144	0.0453	-0.0099	0.0106	0.0006	1.0681
H54 – Se62	0.0110	0.0343	-0.0060	0.0073	0.0012	1.2090
O19 – Se64	0.0152	0.0484	-0.0108	0.0114	0.0006	1.0595
Se57 – O68	0.0138	0.0434	-0.0094	0.0101	0.0007	1.0740
Se64 – H84	0.0124	0.0358	-0.0068	0.0079	0.0010	1.1521
Intermolecular hydrogen bonds						
O19 – H74	0.0053	0.0202	-0.0034	0.0042	0.0008	1.2409
H41 – O68	0.0063	0.0231	-0.0041	0.0049	0.0007	1.1902
H28 – O68	0.0122	0.0389	-0.0097	0.0097	-1.8E-05	0.9981
O24 – H78	0.0122	0.0487	-0.0089	0.0105	0.0016	1.1842
O56 – H84	0.0059	0.0226	-0.0037	0.0047	0.0009	1.2517

interactions is higher. The CPSeNP/PCA4 species is included 23 interactions Se-L with  $\rho_{av} = 0.0125$  and  $\nabla^2\rho_{av} = 0.038138$ .

The second group of non-bonded interactions between CP and PCA is investigated through hydrogen bond. The interaction of H28 ... O68 with  $\nabla^2\rho > 0$ ,  $E_{HB} = -12.82 \text{ kJ mol}^{-1}$ ,  $H_b < 0$ ,  $0.5 < -G_b/V_b < 1$  is related to the medium hydrogen bond (Fig. 3 and Table 3). Four other hydrogen bonds are weak.

The CPSeNP/PCA2 structure is the most unstable configuration. The molecular graph and values of  $-G_b/V_b$ ,  $\rho(r)$ ,  $V_b$ ,  $G_b$ ,  $H_b$ ,  $\nabla^2\rho(r)$  have been presented in Fig. 4 and Table 4, respectively. Similar to CPSeNP/PCA4, Se-L interactions with  $H_b > 0$ ,  $-G_b/V_b >$ ,  $\nabla^2\rho > 0$  related to weak interactions. CPSeNP/PCA10 include 29 Se-L interactions with  $\rho_{av} = 0.0117$  and  $\nabla^2\rho_{av} = 0.0365$ . The interactions between PCA and CP have been investigated through hydrogen bond. The interaction of H75 ... O21 with

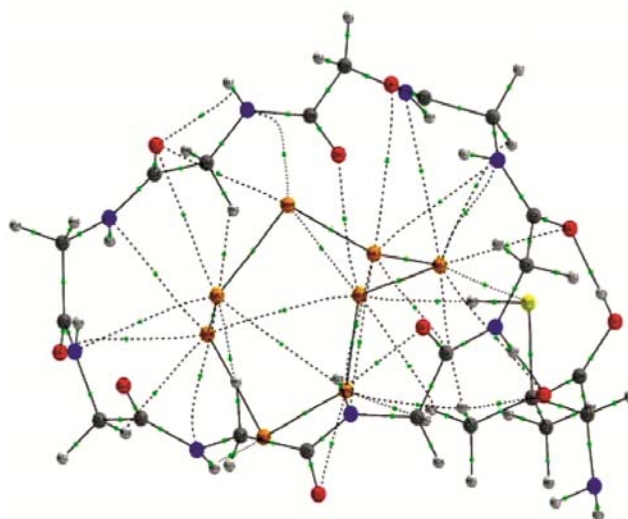


Fig. 4 — QTAIM Molecular graph of CPSeNP/PCA2.

$H_b < 0.5$ ,  $E_{HB} = -55.29 \text{ kJ mol}^{-1}$ ,  $\nabla^2\rho > 0$ ,  $-G_b/V_b < 1$  is related to the medium hydrogen bond and one other hydrogen bond is weak (Table 4, Fig. 4).

Table 4 — Topological parameters in a.u. for CPSeNP/PCA2

Atoms	$\rho(r)$	$\nabla^2\rho(r)$	$V_b$	$G_b$	$H_b$	$-G_b/V_b$
Se–Se interactions						
Se62 – Se63	0.0951	–0.0386	–0.0736	0.0319	–0.0416	0.4343
Se60 – Se63	0.0161	0.0438	–0.0087	0.0098	0.0011	1.1279
Se57 – Se60	0.0150	0.0387	–0.0076	0.0086	0.0010	1.1309
Se57 – Se58	0.1108	–0.0605	–0.0993	0.0420	–0.0572	0.4238
Se57 – Se64	0.1042	–0.0540	–0.0872	0.0368	–0.0503	0.4226
Se61 – Se64	0.0179	0.0450	–0.0094	0.0103	0.0009	1.0960
Se58 – Se59	0.1018	–0.0511	–0.0834	0.0353	–0.0480	0.4233
Se60 – Se61	0.1062	–0.0698	–0.0874	0.0349	–0.0524	0.4001
Se59 – Se60	0.1128	–0.0766	–0.1000	0.0404	–0.0596	0.4042
Se58 – Se61	0.0164	0.0435	–0.0086	0.0097	0.0011	1.1266
Se61 – Se62	0.1114	–0.0732	–0.0985	0.0400	–0.0584	0.4069
Se–L interactions						
N11 – Se57	0.0126	0.0386	–0.0073	0.0085	0.0011	1.1590
N14 – Se57	0.0116	0.0333	–0.0070	0.0076	0.0006	1.0918
N17 – Se58	0.0142	0.0401	–0.0086	0.0093	0.0006	1.0788
C6 – Se63	0.0144	0.0521	–0.0093	0.0111	0.0018	1.1986
N8 – Se63	0.0089	0.0237	–0.0051	0.0055	0.0004	1.0809
N2 – Se63	0.0126	0.0362	–0.0073	0.0082	0.0008	1.1150
H41 – Se57	0.0085	0.0293	–0.0045	0.0059	0.0013	1.2978
N44 – Se64	0.0117	0.0368	–0.0064	0.0078	0.0013	1.2102
N53 – Se62	0.0090	0.0250	–0.0049	0.0055	0.0006	1.1333
O22 – Se58	0.0131	0.0441	–0.0081	0.0096	0.0014	1.1751
H45 – Se58	0.0133	0.0398	–0.0074	0.0087	0.0012	1.1642
H26 – Se59	0.0144	0.0382	–0.0083	0.0089	0.0005	1.0689
H42 – Se60	0.0124	0.0399	–0.0071	0.0085	0.0014	1.1993
O23 – Se60	0.0197	0.0656	–0.0148	0.0156	0.0007	1.0530
O49 – Se61	0.0151	0.0485	–0.0105	0.0113	0.0008	1.0760
H31 – Se62	0.0114	0.0383	–0.0060	0.0078	0.0017	1.2854
N2 – Se62	0.0098	0.0329	–0.0062	0.0072	0.0010	1.1609
O21 – Se62	0.0110	0.0367	–0.0071	0.0081	0.0010	1.1424
O56 – Se63	0.0101	0.0307	–0.0060	0.0068	0.0007	1.1304
Se62 – O71	0.0083	0.0241	–0.0049	0.0054	0.0005	1.1138
Se62 – H80	0.0081	0.0259	–0.0042	0.0053	0.0011	1.2660
Se60 – H80	0.0138	0.0444	–0.0080	0.0095	0.0015	1.1936
Se61 – H79	0.0092	0.0296	–0.0046	0.0060	0.0013	1.2928
Se61 – H78	0.0078	0.0237	–0.0034	0.0046	0.0012	1.3567
Intermolecular hydrogen bonds						
O21 – H75	0.0494	0.1658	–0.0421	0.0417	–0.0003	0.9920
H30 – O71	0.0277	0.0891	–0.0217	0.0220	0.0002	1.0114

## Conclusions

Eleven peptide-selenium nanoparticles CPSeNP have been investigated with PCA anti-cancer drug at M06-2X level of theory in gas phase and water. It was used for cyclic peptide and selenium nanoparticles from cyclooctaglycine and Se8 ring model, respectively. The binding energy values indicate that the CPSeNP/PCA4 function is more appropriate and the interaction between drug-CP and SeNP leads to

more stability. Solvation energies and quantum molecular descriptors show that PCA and SeNP solubility increases in the presence of CP and PCA reactivity increases in the vicinity of CPSeNP. Also, according to the QTAIM studies, PCA can be absorbed on CPSeNP via hydrogen bonding and Se-L interactions (Se-L; L = O, N, C, S, H). Se-L interactions and most hydrogen bonds are related to weak interactions ( $\nabla^2\rho > 0$ ,  $H_b > 0$  and  $-G_b/V_b > 1$ ).

### Supplementary Data

Supplementary Data associated with this article are available in the electronic form at [http://nopr.niscair.res.in/jinfo/ijca/IJCA\\_59A\(01\)43-50\\_SupplData.pdf](http://nopr.niscair.res.in/jinfo/ijca/IJCA_59A(01)43-50_SupplData.pdf).

### Acknowledgement

The authors thank the Research Centre for Animal Development Applied Biology for allocation of computer time.

### References

- De Jong W H & Borm P J A, *Int J Nanomed*, 3 (2008) 133.
- Arruebo M, *Wiley Interdiscip Rev Nanomed Nanobiotechnol*, 4 (2012) 16.
- Maharramov A M, Alieva I N, Abbasova G D, Ramazanov M, Nabiyev N S & Saboktakin M R, *Dig J Nanomater Biostruct*, 6 (2011) 419.
- Tang F, Li L & Chen D, *Adv Mater*, 24 (2012) 1504.
- Llevot A & Astruc D, *Chem Soc Rev*, 41 (2012) 242.
- Singh R K & Kim H W, *Tissue Eng Regen Med*, 10 (2013) 296.
- Huang H C, Barua S, Sharma G, Dey S K & Rege K, *J Controll Release*, 155 (2011) 344.
- Xu Z P, Zeng Q H, Lu G Q & Yu A B, *Chem Eng Sci*, 61 (2006) 1027.
- Deka K, Kumar J, Bhowmick A, Banu S & Das D K, *Ind J Chem Sec A*, 57A (2018) 485.
- Hartgerink J D, Clark T D & Ghadiri M R, *Chem Eur J*, 4 (1998) 1367.
- Sánchez-Quesada J, Sun Kim H & Ghadiri M R, *Angew Chem Int Ed*, 40 (2001) 2503.
- Fernandez-Lopez S, Kim H-S, Choi E C, Delgado M, Granja J R, Khasanov A, Kraehenbuehl K, Long G, Weinberger D A & Wilcoxon K M, *Nature*, 412 (2001) 452.
- Ortiz-Acevedo A, Xie H, Zorbass V, Sampson W M, Dalton A B, Baughman R H, Draper R K, Musselman I H & Dieckmann G R, *J Am Chem Soc*, 127 (2005) 9512.
- Khavani M, Izadyar M & Housaindokht M R, *J Mol Graphics Modell*, 71 (2017) 28.
- Mandal D, Nasrolahi Shirazi A & Parang K, *Angew Chem Int Ed*, 50 (2011) 9633.
- Oh D, Nasrolahi Shirazi A, Northup K, Sullivan B, Tiwari R K, Bisoffi M & Parang K, *Mol Pharm*, 11 (2014) 2845.
- Nasrolahi Shirazi A, Mandal D, Tiwari R K, Guo L, Lu W & Parang K, *Mol Pharm*, 10 (2012) 500.
- Peisach J & Blumberg W, *Mol Pharmacol*, 5 (1969) 200.
- Camp A, *J Rheumatol Suppl*, 7 (1980) 103.
- Wadhwa S & Mumper R J, *Cancer Lett*, 337 (2013) 8.
- Khorsand A, Jamehbozorgi S, Ghiasi R & Rezvani M, *Physica E*, 72 (2015) 120.
- Wadhwa S & Mumper R J, *Mol Pharm*, 7 (2010) 854.
- Gupte A, Wadhwa S & Mumper R J, *Bioconjugate Chem*, 19 (2008) 1382.
- Zhang Y, Chan H F & Leong K W, *Adv Drug Deliv Rev*, 65 (2013) 104.
- Andrade F, Rafael D, Videira M, Ferreira D, Sosnik A & Sarmento B, *Adv Drug Deliv Rev*, 65 (2013) 1816.
- Mei L, Zhang Z, Zhao L, Huang L, Yang X-L, Tang J & Feng S-S, *Adv Drug Deliv Rev*, 65 (2013) 880.
- Silhol M, Tyagi M, Giacca M, Lebleu B & Vivès E, *Eur J Biochem*, 269 (2002) 494.
- Thorén P E, Persson D, Isakson P, Goksör M, Önfelt A & Nordén B, *Biochem Biophys Res Commun*, 307 (2003) 100.
- Yang G & Zhou R, *J Trace Elem Electro Health Dis*, 8 (1994) 159.
- Nasrolahi Shirazi A, Tiwari R K, Oh D, Sullivan B, Kumar A, Beni Y A & Parang K, *Mol Pharm*, 11 (2014) 3631.
- Sarin L, Sanchez V C, Yan A, Kane A B & Hurt R H, *Adv Mater*, 22 (2010) 5207.
- Wang D, Taylor E W, Wang Y, Wan X & Zhang J, *Int J Nanomed*, 7 (2012) 1711.
- Mohammad-Hasani E, Beyramabadi S A & Pordel M, *Ind J Chem Sec A*, 56A (2017) 626.
- Kamel M, Raissi H, Morsali A & Shahabi M, *Appl Surf Sci*, 434 (2018) 492.
- Khorram R, Raissi H & Morsali A, *J Mol Liq*, 240 (2017) 87.
- Saikia N & Deka R C, *Struct Chem*, 25 (2014) 593.
- Zheng Y B, Kiraly B & Huang T J, *Nanomedicine*, 5 (2010) 1309.
- Linko V, Ora A & Kostianinen M A, *Trends Biotechnol*, 33 (2015) 586.
- Hesabi M & Behjatmanesh-Ardakani R, *Appl Surf Sci*, 427 (2018) 112.
- Kamel M, Raissi H & Morsali A, *J Mol Liq*, 248 (2017) 490.
- Hafizi H, Chermahini A N, Mohammadnezhad G & Teimouri A, *Appl Surf Sci*, 329 (2015) 87.
- Teymouri M, Morsali A, Bozorgmehr M R & Beyramabadi S A, *Bull Korean Chem Soc*, 38 (2017) 869.
- Arsawang U, Saengsawang O, Rungrotmongkol T, Sornmee P, Wittayanarakul K, Remsungnen T & Hannongbua S, *J Mol Graph Modell*, 29 (2011) 591.
- Lotfi M, Morsali A & Bozorgmehr M R, *Appl Surf Sci*, 462 (2018) 720.
- Jalayeri E, Morsali A & Bozorgmehr M R, *Ind J Chem Sec A*, 55A (2016) 1202.
- Zhao Y, Schultz N E & Truhlar D G, *J Chem Theory Comput*, 2 (2006) 364.
- Zhao Y & Truhlar D G, *J Chem Phys*, 125 (2006) 194101.
- Frisch M, Trucks G, Schlegel H, Scuseria G, Robb M, Cheeseman J, Scalmani G, Barone V, Mennucci B & Petersson G, *Gaussian 09, revision B.01. Gaussian, Inc., Wallingford, CT* (2009).
- Cammi R & Tomasi J, *J Comp Chem*, 16 (1995) 1449.
- Tomasi J & Persico M, *Chem Rev*, 94 (1994) 2027.
- Parr R G, Szentpaly L V & Liu S, *J Am Chem Soc*, 121 (1999) 1922.
- Keith T A, *TK Gristmill Software, Overland Park KS, USA* (2013).
- Bader R F, *Chem Rev*, 91 (1991) 893.
- Poteau R & Trinquier G, *J Am Chem Soc*, 127 (2005) 13875.
- Li I L, Ruan S, Li Z, Zhai J & Tang Z, *Appl Phys Lett*, 87 (2005) 071902.
- He J, Lv W, Chen Y, Wen K, Xu C, Zhang W, Li Y, Qin W & He W, *ACS nano*, 11 (2017) 8144.
- Rozas I, Alkorta I & Elguero J, *J Am Chem Soc*, 122 (2000) 11154.
- Espinosa E, Souhassou M, Lachekar H & Lecomte C, *Acta Crystall Sect B: Struct Sci*, 55 (1999) 563.